# SPACE CHARGE

*K. Schindl*
CERN, CH-1211 Geneva 23
E-mail: Karlheinz.Schindl@cern.ch

**Abstract**
The Coulomb forces between the charged particles of a high-intensity beam in an accelerator create a self-field which acts on the particles inside the beam like a distributed lens, defocusing in both transverse planes. A beam moving with speed $v$ is accompanied by a magnetic field which partially cancels the electrostatic defocusing effect, with complete cancellation at $c$, the speed of light. The effect of this 'direct space charge' is evaluated for transport lines and synchrotrons where the number of betatron oscillations per machine turn, $Q$, is reduced by $\Delta Q$. In a real accelerator, the beam is also influenced by the environment (beam pipe, magnets, etc.) which generates 'indirect' space charge effects. For a smooth and perfectly conducting wall, they can easily be evaluated by introducing image charges and currents. These 'image effects' do not cancel when $v$ approaches $c$, thus they become dominant for high-energy synchrotrons. Each particle in the beam has its particular incoherent tune $Q$ and incoherent tune shift $\Delta Q$. If the beam moves as a whole, so the centre of mass executes a coherent betatron oscillation, image charges and currents caused by the beam pipe move as well, leading to coherent tune shifts which also depend on the beam intensity. For a realistic beam, the incoherent tune of a given particle depends on its betatron amplitude and position in the bunch, leading to a tune spread (rather than a tune shift) which occupies a large area in the tune diagram of low-energy machines. The 'space-charge limit' of a synchrotron may be overcome by increasing its injection energy; various systems which have actually been built are presented.

## 1. INTRODUCTION

Space charge is the simplest and most fundamental of the collective effects whose impact generally is proportional to the beam intensity. The charge and current of the beam create self-fields and image fields which alter its dynamic behaviour and influence the single-particle motion as well as coherent oscillations of the beam as a whole. The paper concentrates on changes of the betatron tune in synchrotrons for simple cases which can readily be calculated; the emphasis is on low-energy (more precisely: low-$\gamma$) machines where space charge represents a fundamental intensity limitation. The lecture this paper is based upon is intended for physicists, engineers and senior technicians who are not familiar with collective effects and is meant as an introduction to the subject. The reader is assumed to be familiar with the basic laws of classical electrodynamics; SI units are used throughout. In many respects, the paper is inspired by earlier CAS lectures [1–3]. Reference [2] also covers the particular intricacies of high-energy machines (which in this context include all electron synchrotrons) and more complex cases. Methods for measuring space-charge tune shifts/spreads in synchrotrons are presented in Ref. [3].

## 2. DIRECT SPACE CHARGE (SELF-FIELDS)

Consider two particles of equal charge +e (Fig. 1). At rest, they experience the repulsion due to the Coulomb force. When travelling with velocity $v = \beta c$, they represent two parallel currents $I = ve$ which attract each other by the effect of their magnetic fields. The diagram shows that the overall effect is still repulsive but decreases with the speed; special relativity implies that the forces become equal at the speed of light and thus cancel.

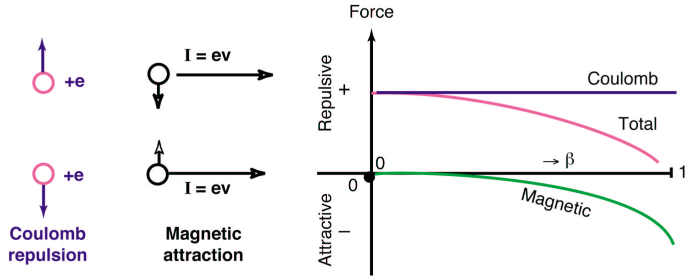


Fig. 1: Coulomb repulsion and magnetic attraction between two particles of equal charge, at rest and travelling

Now consider many charged particles travelling in an unbunched beam with circular cross section (Fig. 2). The Coulomb repulsion pushes the test particle away from the beam centre; the overall force is zero in the beam centre and increases towards the edge. This behaviour applies also to the test particle in a travelling beam, represented by parallel currents, except that the magnetic force vector is directed towards the beam centre.

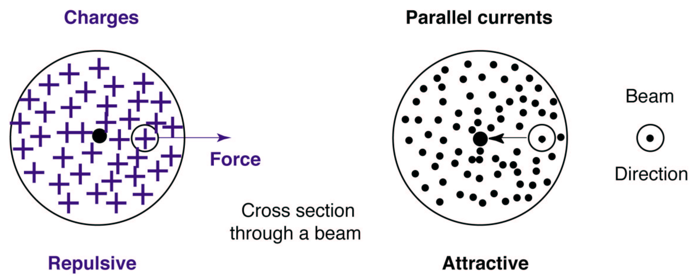


Fig. 2: Electrostatic and magnetic forces on a test particle within a cylindrical unbunched beam

### 2.1. The self-field

An unbunched beam of circular cross section (radius $a$) and uniform charge density $\eta$ [Cb/m$^3$] moves with constant velocity $v = \beta c$. It has a line charge density (charge per unit length [Cb/m]) of $\lambda = \pi a^2 \eta$, a current density [A/m$^2$] of $J = \beta c \eta$, and a total current of $I = \beta c \lambda$. Figure 3 represents the beam; in the following, the electric $\vec{\mathrm{E}}$ and magnetic $\vec{\mathrm{B}}$ fields on the surface of a cylinder with radius $r < a$ are calculated (using polar coordinates $r,\ \phi$). Due to symmetry, the electric field has just a radial component ($E_\mathrm{r}$), while the magnetic field lines are just circles around the cylinder ($B_\phi$ component only).

$E_\mathrm{r}$ is calculated from the Maxwell equation

$$\mathrm{div}\ \vec{\mathrm{E}} = \frac{\eta}{\varepsilon_0} \tag{1}$$

and its integral form, Gauss' law (integration over volume and surface of cylinder with radius $r$ and length $l$)

$$\iiint \mathrm{div}\ \vec{\mathrm{E}} \mathrm{d}V = \iint \vec{\mathrm{E}} \mathrm{d}\vec{\mathrm{S}} \tag{2}$$

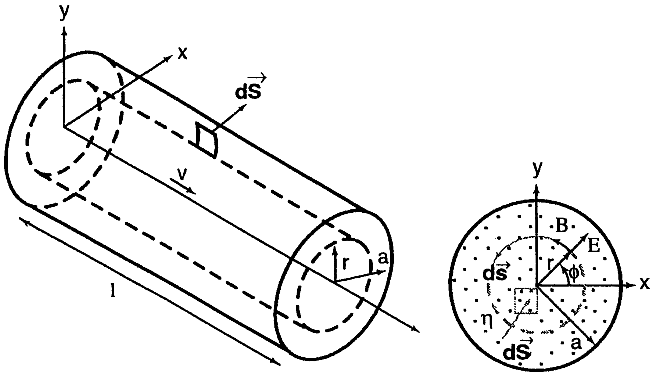


Fig. 3: Uniformly charged cylinder of length $l$ (left) and its circular cross section (right) with symbols used in Eqs. (1)–(8)

where $\mathrm{d}V$ is a volume element inside the cylinder, and $\mathrm{d}\vec{\mathrm{S}}$ an element of its surface (Fig. 3), yielding

$$\pi l r^2 \frac{\eta}{\varepsilon_0} = 2\pi l r E_\mathrm{r} \tag{3}$$

from which one can derive the radial electric field

$$E_\mathrm{r} = \frac{I}{2\pi\varepsilon_0 \beta c} \frac{r}{a^2} \,. \tag{4}$$

Similarly, the azimuthal magnetic field $B_\phi$ is determined from another Maxwell equation

$$\mathrm{curl}\, \vec{\mathrm{B}} = \mu_0 \, \vec{\mathrm{J}} \tag{5}$$

and its integral form, Stokes' law

$$\oint \vec{\mathrm{B}} \mathrm{d}\vec{\mathrm{s}} = \iint \; \mathrm{curl}\, \vec{\mathrm{B}} \mathrm{d}\vec{\mathrm{S}} \,, \tag{6}$$

where $\mathrm{d}\vec{\mathrm{s}}$ is a path element in the cross section along the circle with radius $r$, and $\mathrm{d}\vec{\mathrm{S}}$ a surface element within this circle (Fig. 3). The integrals (6) over the cylinder of radius $r$ and length $l$ result in

$$2\pi r B_\phi = \mu_0 \pi r^2 \beta c \eta \tag{7}$$

yielding the magnetic field

$$B_\phi = \frac{I}{2\pi\varepsilon_0 c^2} \frac{r}{a^2} \,. \tag{8}$$

Indeed, both electric and magnetic fields vanish at $r$ = 0, and both increase linearly with $r$ up to the edge of the cylinder $(r = a)$.

### 2.2. The forces

These fields exert a force $\vec{\mathrm{F}}$ on a test particles at radius $r$ (the magnetic force is sketched in Fig. 4) which is now calculated:

$$\vec{\mathrm{F}} = e(\vec{\mathrm{E}} + [\vec{\mathrm{v}} \times \vec{\mathrm{B}}]) \tag{9}$$

For the geometry under consideration Eq. (9) simplifies to

$$F_\mathrm{r} = e(E_\mathrm{r} - v_\mathrm{s} B_\phi) \tag{10}$$

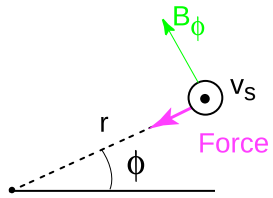


Fig. 4: Magnetic force on a test particle at radius $r$ travelling with velocity $v_{\mathrm{s}}$ due to an azimuthal magnetic field $B_\phi$

indicating that the force vector has a purely radial component $F_{\mathrm{r}}$. Inserting $E_{\mathrm{r}}$ and $B_\phi$ from equations (4) and (8) one gets for the radial force on the test particle at radius $r$

$$F_{\mathrm{r}} = \frac{eI}{2\pi\varepsilon_0\beta c}(1-\beta^2)\frac{r}{a^2} = \frac{eI}{2\pi\varepsilon_0\beta c}\frac{1}{\gamma^2}\frac{r}{a^2}\,. \tag{11}$$

In the (1 - $\beta^2$) term, the '1' represents the electric force, and the $\beta^2$ the magnetic one, and indeed they cancel at $\beta$ = 1; it is replaced by 1/$\gamma^2$ in Eq. (11). Replacing $r$ by the transverse coordinates $x$, $y$ results in the horizontal ($F_{\mathrm{x}}$) and vertical ($F_{\mathrm{y}}$) forces which are linear in $x$ and $y$, respectively:

$$F_{\mathrm{x}} = \frac{eI}{2\pi\varepsilon_0 c\beta\gamma^2 a^2}\,x\,, \qquad F_{\mathrm{y}} = \frac{eI}{2\pi\varepsilon_0 c\beta\gamma^2 a^2}\,y\,. \tag{12}$$

It is instructive to compare the focusing effects of a quadrupole with the uniform high-intensity beam for which Eq. (12) applies. Figure 5 shows the force $F_{\mathrm{x}}$ vs. $x$ for a (horizontally focusing) quadrupole, and for a space-charge dominated uniform beam. While the quadrupole is focusing in one and defocusing in the other plane, direct space charge leads to defocusing in both planes.

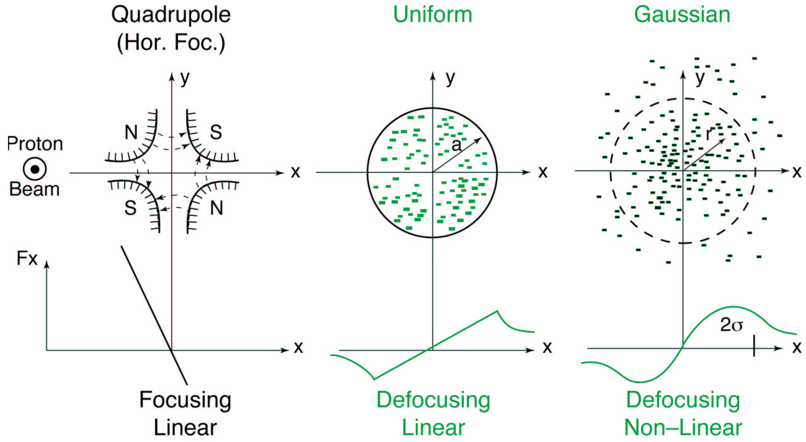


Fig. 5: Focusing/defocusing force $F_{\mathrm{x}}$ vs. $x$ of a quadrupole (left), and of space-charge dominated beams: uniform (centre) and Gaussian (right)

### 2.3. Beam transport with space charge

A FODO transport line is described by Hill's equation

$$x'' + K(s)\,x = 0\,, \tag{13}$$

where $K(s)$ denotes the normalised gradients (positive if focusing, negative if defocusing) of the quadrupoles along the beam path $s$ (here for the horizontal plane). A perturbation term $K_{\mathrm{SC}}(s)$ describes the (continuous) defocusing action of space charge:

$$x'' + (K(s) + K_{\mathrm{SC}}\,(s))\,x = 0\,. \tag{14}$$

$K_{\rm SC}$ is derived by expressing $x''$ in terms of transverse acceleration $\mathrm{d}^2x/\mathrm{d}t^2$ and thus of the force $F_{\rm x}$ [Eq. (12)]

$$x'' = \frac{\mathrm{d}^2\,x}{\mathrm{d}s^2} = \frac{1}{\beta^2c^2}\frac{\mathrm{d}^2\,x}{\mathrm{d}t^2} = \frac{\ddot{\rm x}}{\beta^2c^2} = \frac{1}{\beta^2c^2}\frac{F_{\rm x}}{m_0\gamma} = \frac{2r_0I}{ea^2\beta^3\gamma^3c}\,x\,, \tag{15}$$

where $r_0 = e^2/(4\pi\varepsilon_0 m_0c^2)$ is the classical particle radius, $1.54\times10^{-18}$ m for protons. Hill's equation with space charge (for an unbunched beam with circular cross section and constant charge density) is then

$$x'' + \left(K(s) - \frac{2r_0I}{ea^2\beta^3\gamma^3c}\right)x = 0\,. \tag{16}$$

Note the negative sign of the space charge term, reducing the overall focusing of the FODO sequence.

### 2.4. Direct space charge in a synchrotron: Incoherent tune shift

The direct space charge leads to defocusing in either plane, and therefore one would expect that particles in a high-intensity beam will experience a lowering of their betatron tunes $Q$ by $\Delta Q$. The calculation below applies to the simplest (pretty unrealistic) case: unbunched beam, circular cross section everywhere in the accelerator, constant charge density.

Applying Eq. (13) to a synchrotron lattice will yield the unperturbed horizontal $Q_{\rm x0}$, while Eq. (16) introduces a space-charge defocusing $\Delta Q_{\rm x}$ which is readily calculated [4] by integrating the weighted gradient errors around the circumference $2\pi R$:

$$\Delta Q_{\rm x} = \frac{1}{4\pi}\int_0^{2\pi R} K_{\rm x}(s)\beta_{\rm x}(s)\mathrm{d}s = \frac{1}{4\pi}\int_0^{2\pi R} K_{\rm SC}(s)\beta_{\rm x}(s)\mathrm{d}s\,. \tag{17}$$

Taking $K_{\rm SC}(s)$ from Eq. (16) yields

$$\Delta Q_{\rm x} = -\frac{1}{4\pi}\int_0^{2\pi R}\frac{2r_0I}{e\beta^3\gamma^3c}\frac{\beta_{\rm x}(s)}{a^2}\,\mathrm{d}s = -\frac{r_0\,RI}{e\beta^3\gamma^3c}\left\langle\frac{\beta_{\rm x}(s)}{a^2(s)}\right\rangle\,. \tag{18}$$

The term $\langle\beta_{\rm x}(s)/a^2(s)\rangle$ (remember: $a$ is the beam size) is just $1/E_{\rm x}$, the inverse of the horizontal emittance, and thus an invariant. Replacing $I$ by $Ne\beta c/(2\pi R)$ (with $N$ the number of particles in the accelerator) and extending to the vertical plane $(y)$ one gets for the direct space-charge tune shift

$$\Delta Q_{\rm x,y} = -\frac{r_0N}{2\pi E_{\rm x,y}\beta^2\gamma^3}\,. \tag{19}$$

$E_{\rm x,y}$ is the transverse emittance in either plane containing 100% of the particles. The main features are:

- the tune shift is proportional to the intensity;
- it scales with $1/\gamma^3$, so negligible for all electron synchrotrons, and very small for proton synchrotrons beyond $\sim$ 10 GeV;
- it does not depend on the machine radius $R$.

### 2.5. Direct space charge for a uniform beam with elliptic beam cross section

For this geometry (Fig. 6), Maxwell's Eqs. (1) and (5) are satisfied by the electric and magnetic fields $\vec{\rm E}$ and $\vec{\rm B}$

$$\vec{\rm E} = \frac{I}{\pi\varepsilon_0(a+b)\beta c}\left(\frac{x}{a}\,,\frac{y}{b}\,,0\right)\,,\qquad \vec{\rm B} = \frac{\mu_0I}{\pi(a+b)}\left(-\frac{y}{b}\,,\frac{x}{a}\,,0\right)\,. \tag{20}$$

A particle at position $(x,\ y)$ inside the beam will experience a force

$$\vec{\rm F} = e(\vec{\rm E} + [\vec{\rm v}\times\vec{\rm B}]) = \frac{eI}{\pi\varepsilon_0\beta c\gamma^2(a+b)}\left(\frac{x}{a}\,,\frac{y}{b}\,,0\right) \tag{21}$$

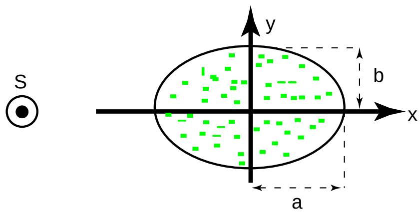


Fig. 6: Cross section through an elliptic beam with constant charge density $\eta$

from which, following the reasoning behind Eq. (15), the space-charge defocusing term $K_{\mathrm{SC,y}}$ (here for the vertical plane)

$$K_{\mathrm{SC,y}} = -\frac{F_{\mathrm{y}}}{m_0 \gamma \beta^2 c^2} \frac{1}{y} = -\frac{4 r_0 I}{e b (a+b) \beta^3 \gamma^3 c} \tag{22}$$

and the vertical tune shift

$$\Delta Q_{\mathrm{y}} = \frac{1}{4\pi} \int_0^{2\pi R} K_{\mathrm{SC,y}}(s) \beta_{\mathrm{y}}(s) \mathrm{d}s = -\frac{2 r_0 I}{e c \beta^3 \gamma^3 E_{\mathrm{y}}} \left\langle \frac{b}{a+b} \right\rangle \tag{23}$$

can be determined. One then approximates the averaging of term $\langle b/(a+b) \rangle$

$$\left\langle \frac{b}{a+b} \right\rangle \cong \frac{1}{\langle \frac{a}{b} + 1 \rangle} = \frac{1}{\sqrt{\langle \beta_{\mathrm{x}} \rangle E_{\mathrm{x}} / \langle \beta_{\mathrm{y}} \rangle E_{\mathrm{y}}} + 1} \tag{24}$$

to obtain the vertical direct space charge tune shift of a uniform beam with elliptic cross section

$$\Delta Q_{\mathrm{y}} \cong -\frac{r_0 N}{2\pi E_{\mathrm{y}} \beta^2 \gamma^3} \frac{2}{(1 + \sqrt{\bar{\beta}_{\mathrm{x}} E_{\mathrm{x}} / \bar{\beta}_{\mathrm{y}} E_{\mathrm{y}}})} \,. \tag{25}$$

Exchanging all $x$'s and $y$'s, one obtains the horizontal shift $\Delta Q_{\mathrm{x}}$. Typical synchrotrons feature small vertical gap sizes in the dipoles and hence $E_{\mathrm{y}} < E_{\mathrm{x}}$, which in turn gives rise to $\Delta Q_{\mathrm{y}} > \Delta Q_{\mathrm{x}}$.

### 2.6. Direct space charge for a non-uniform beam

In the preceding sections only beams with constant charge density $\eta$ are considered. In what follows, a simple — and rather realistic — example for a non-uniform distribution, namely a bi-Gaussian density in the circular beam cross section, is analysed. The distribution is

$$\eta(r) = \frac{I}{2\pi \beta c \sigma^2} \, e^{-r^2/2\sigma^2} \,, \qquad r = \sqrt{x^2 + y^2} \,, \tag{26}$$

where $\sigma$ denotes the r.m.s. value of the distribution projected on the $x$- (or $y$-) axis. Maxwell's equations (1) and (5) are satisfied by the following expressions for $E_{\mathrm{r}}$ and $B_\phi$ (the other field components vanish because of circular symmetry) as can be readily verified:

$$E_{\mathrm{r}} = \frac{I}{2\pi \varepsilon_0 \beta c} \frac{1}{r} \left(1 - e^{-r^2/2\sigma^2}\right) \,, \qquad B_\phi = \frac{I}{2\pi \varepsilon_0 c^2} \frac{1}{r} \left(1 - e^{-r^2/2\sigma^2}\right) \,. \tag{27}$$

This yields a radial force

$$F_{\mathrm{r}}(r) = \frac{eI}{2\pi \varepsilon_0 \beta c \gamma^2} \frac{1}{r} \left(1 - e^{-r^2/2\sigma^2}\right) \,, \tag{28}$$

which is no longer linear in $r$, thus the defocusing becomes betatron-amplitude dependent (Fig. 5, right). It is instructive to linearise the force for small $r$ (near the beam centre)

$$F_{\mathrm{r}}(r) = \frac{eI}{2\pi\varepsilon_0\beta\gamma^2 c}\frac{1}{r}\left(1 - 1 + \frac{r^2}{2\sigma^2} - \ldots\right) \approx \frac{eI}{2\pi\varepsilon_0\beta\gamma^2 c}\frac{r}{2\sigma^2}\,,$$

$$F_{\mathrm{y}}(y) \approx \frac{eI}{2\pi\varepsilon_0\beta\gamma^2 c}\frac{y}{2\sigma^2}\,, \tag{29}$$

resulting in a small-amplitude (vertical) tune shift of

$$\Delta Q_{\mathrm{y}} = -\frac{r_0 IR}{ec\beta^3\gamma^3}\left\langle\frac{\beta_{\mathrm{y}}}{2\sigma^2}\right\rangle = -\frac{r_0 N}{2\pi\beta^2\gamma^3}\,\frac{2}{E_{\mathrm{y}}}\ \text{for}\ r \ll \sigma \tag{30}$$

with $E_{\mathrm{y}} = 4\sigma^2/\beta_{\mathrm{y}}$, the 95% emittance.

This is twice the figure of a uniform beam of the same cross-sectional size and intensity. The important conclusions are: (i) for given emittances and intensity, a uniformly distributed beam gives the smallest possible direct space-charge tune shift; (ii) a — more realistic — non-uniform transverse charge distribution features a betatron amplitude-dependent de-tuning, hence a tune *spread* rather than a shift. In beams with transverse density profiles resembling a Gaussian which are typical for hadron cooler rings, small-amplitude particles suffer the largest tune depression.

## 3. TUNE SHIFT WITH WALL EFFECTS

In Section 2, the impact of the self-field created by the beam alone was investigated, resulting in 'direct' space-charge tune shifts and spreads. A real accelerator, however, consists of a vacuum pipe, accelerator gaps, magnets, beam diagnostics, and a high-intensity beam induces surface charges or currents into this environment that act back on the beam, possibly resulting in an 'indirect' space-charge tune shift. The basic effect is demonstrated below for a very simple geometry (Fig. 7) where the beam is best represented by a line charge $\lambda$ of infinite length.

### 3.1. 'Incoherent' tune shift due to conductive walls

The boundary condition on a perfectly conducting plate (E-parallel = $E_{\|}$ = 0) is satisfied by introducing 'image' line charges of negative sign as shown in Fig. 7 (right). The beam, whose barycenter is halfway between two parallel conducting plates, gives rise to an infinite number of image line charges of alternating sign at positions 2h, 4h, 6h,....–2h, –4h,.... (see Fig. 7 left). A test line charge positioned vertically off-centred by y, but still inside the beam, will be subject to an infinite sum of electric fields; is it non-zero?

The electric field generated by a line charge $\lambda$ at distance $d$ (Fig. 8) is

$$E_{\mathrm{y}} = \frac{\lambda}{2\pi\varepsilon_0}\,\frac{1}{d} \tag{31}$$

Applying Eq. (31) to the first pair of image line charges, positioned at 2h, –2h, yields the vertical field at point y generated by the two images, $E_{\mathrm{ily}}$; more generally, the $n^{\mathrm{th}}$ pair of line charges, positioned at 2nh, –2nh, results in $E_{\mathrm{iny}}$:

$$\begin{aligned} E_{\mathrm{ily}} &= \frac{\lambda}{2\pi\varepsilon_0}\left(\frac{1}{2h-y} - \frac{1}{2h+y}\right)\,, \\ E_{\mathrm{iny}} &= (-1)^{\mathrm{n}}\frac{\lambda}{2\pi\varepsilon_0}\left(\frac{1}{2nh+y} - \frac{1}{2nh-y}\right) = (-1)^{\mathrm{n}}\frac{\lambda}{4\pi\varepsilon_0}\frac{y}{n^2h^2}\,. \end{aligned} \tag{32}$$

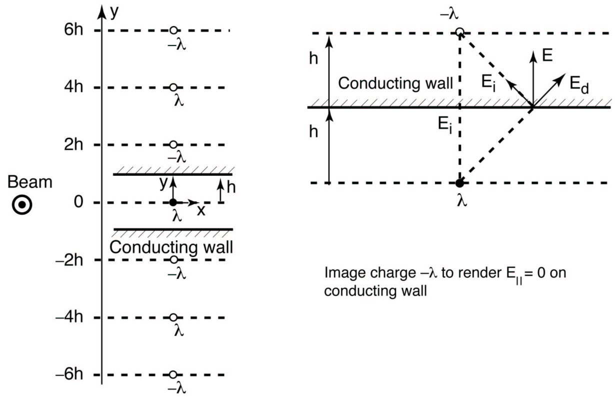


Fig. 7: A line charge $\lambda$, representing the particle beam, between parallel conducting plates of distance 2h (left). Electric field components parallel to the conducting plate have to be zero: this is achieved by introducing negative image line charges (right).

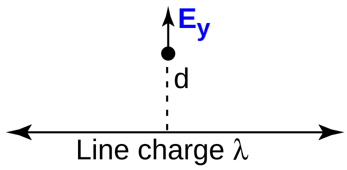


Fig. 8: Electric field created at distance $d$ by a line charge extending to infinity

The total vertical electric field $E_{\mathrm{iy}}$ is readily obtained by summing $E_{\mathrm{iny}}$ from $n$ = 1 to infinity

$$E_{\mathrm{iy}} = \sum_{1}^{\infty} E_{\mathrm{iny}} = \frac{\lambda}{4\pi\varepsilon_0 h^2} \sum_{1}^{\infty} \frac{(-1)^{\mathrm{n}}}{n^2}\, y = \frac{\lambda}{4\pi\varepsilon_0 h^2}\frac{\pi^2}{12} y \tag{33}$$

by making use of the expression

$$\sum_{1}^{\infty} \frac{(-1)^{\mathrm{n}}}{n^2} = \frac{\pi^2}{12} \,. \tag{34}$$

The vertical electric field due to the images is linear in $y$ (vertical distance of the test particle). Between the parallel plates, there are no image charges, therefore Eq. (1) simplifies to div $\vec{\mathrm{E}}_{\mathrm{i}}$ = 0 from which the component $E_{\mathrm{ix}}$ as well as the forces in both $y$ and $x$ directions are derived:

$$\begin{aligned} \mathrm{div}\,\vec{\mathrm{E}}_{\mathrm{i}} &= \frac{\partial E_{\mathrm{ix}}}{\partial x} + \frac{\partial E_{\mathrm{iy}}}{\partial y} = 0 \qquad \Longrightarrow \qquad & E_{\mathrm{ix}} = -\frac{\lambda}{4\pi\varepsilon_0 h^2}\frac{\pi^2}{12}\, x \,, \\ F_{\mathrm{iy}} &= \frac{e\lambda}{\pi\varepsilon_0 h^2}\frac{\pi^2}{48}\, y \,, & F_{\mathrm{ix}} = -\frac{e\lambda}{\pi\varepsilon_0 h^2}\frac{\pi^2}{48} x \,. \end{aligned} \tag{35}$$

Following the procedure outlined in Eqs. (15) and (17) which links the force to the $Q$-shift, one obtains — together with the direct space-charge effect [Eq. (18)] — the total *incoherent* tune shift of a round beam between parallel conducting walls

$$\begin{aligned} \Delta Q_{\mathrm{x}} &= -\frac{2r_0 IR\langle\beta_{\mathrm{x}}\rangle}{ec\beta^3\gamma}\left(\underbrace{\frac{1}{2\langle a^2\rangle\gamma^2}}_{\text{direct}} - \underbrace{\frac{\pi^2}{48h^2}}_{\text{image}}\right) \\ \Delta Q_{\mathrm{y}} &= -\frac{2r_0\, IR\langle\beta_{\mathrm{y}}\rangle}{ec\beta^3\gamma}\left(\frac{1}{2\langle a^2\rangle\gamma^2} + \frac{\pi^2}{48h^2}\right) . \end{aligned} \tag{36}$$

Inspection of Eq. (36) reveals a few salient features:

- the electric image field is vertically defocusing, but horizontally focusing (sign of image term changes), which by the way is not just a feature of this particular geometry, but is typical for most synchrotrons with their rather flattish vacuum pipes;
- the field is larger for small chamber height $h$;
- Image effects decrease with $1/\gamma$, much slower than the direct space-charge term ($1/\gamma^3$), and thus are of some concern for electron and high-energy proton machines.

The conductive beam pipe leads to mirror (line) charges as presented above. But the beam travels and represents a d.c. beam current accompanied by an azimuthal d.c. magnetic field which is not shielded by the beam pipe. The magnetic field lines are influenced by ferromagnetic boundaries such as magnets; their effect may be represented by mirror currents, from which an incoherent tune shift due to magnetic images can be calculated (not done here, but the magnetic image coefficients are compiled in Table 1, see later).

### 3.2. 'Coherent' tune shift

The term *'incoherent'* has sneaked into the last paragraph, and now it says: *'coherent'*. What do these terms mean?

- *Incoherent* motion: the beam consists of many particles, each of which moves inside the beam with its individual betatron amplitude, phase, and even tune Q (under the influence of direct space charge). Amplitude and phase are distributed at random over all particles. Except for low-intensity beams, an outside observer (using a position monitor at some azimuth in the synchrotron) does not see any of this random betatron motion. The beam and its centre of gravity — and thus the source of the direct space-charge field — do not move (static beam, Fig. 9).
- *Coherent* motion: A static beam is given a transverse fast deflection ($<$ 1 turn) and starts to perform betatron oscillations as a whole (Fig. 10). This is readily observed by a position monitor. Note that the source of the direct space charge is now moving: individual particles still continue their incoherent motion around the common coherent trajectory and still experience their incoherent tune shifts as well.

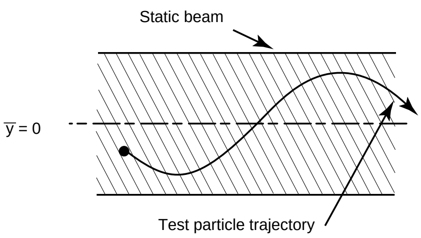


Fig. 9: Incoherent betatron motion of a test particle inside a static beam with its centre of mass at rest.

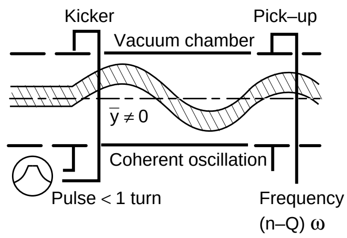


Fig. 10: Coherent betatron motion of the whole beam after having experienced a transverse kick.

In the presence of the accelerator environment, the coherently oscillating beam induces image charges/currents which are oscillating as well. This leads to a *coherent tune shift* as is demonstrated in what follows for a simple geometry: a round, perfectly-conducting beam pipe. Figure 11 shows a beam with line charge $\lambda$ and radius $a$ performing coherent oscillations of its centre of mass $\bar{x}$ inside the round beam pipe with radius $\rho$ ($a \ll \rho$). The displaced line charge $\lambda$ induces surface charges on the inside of the beam pipe which can be represented by an image line charge $-\lambda$ at distance $b$, where

$$b = \frac{\rho^2}{\bar{x}} \tag{37}$$

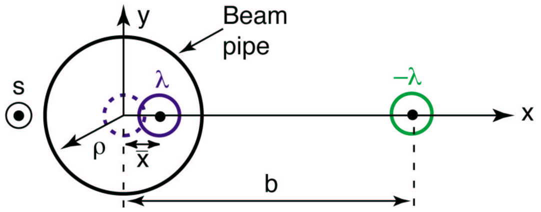


Fig. 11: Coherent oscillation of the beam inside a circular, perfectly conducting beam pipe, and its (oscillating) image charge.

holds [1].

The image charge pulls the beam away from the centre of the beam pipe: its effect is defocusing. The horizontal electric image field $E_{\rm ix}$ and the horizontal force $F_{\rm ix}$ are

$$E_{\rm ix}(\bar{x}) = \frac{\lambda}{2\pi\varepsilon_0}\frac{1}{b-\bar{x}} \approx \frac{\lambda}{2\pi\varepsilon_0}\frac{1}{b} = \frac{\lambda}{2\pi\varepsilon_0}\frac{1}{\rho^2}\bar{x}$$

$$F_{\rm ix}(\bar{x}) = \frac{e\lambda}{2\pi\varepsilon_0}\frac{1}{\rho^2}\bar{x} \tag{38}$$

For symmetry reasons with this particular geometry, the vertical field and force, $E_{\rm iy}$ and $F_{\rm iy}$, are the same as the horizontal ones, and one obtains a *coherent* tune shift of

$$\Delta Q_{\rm x,y,coh.} = -\frac{r_0 R\langle\beta_{\rm x,y}\rangle I}{ec\beta^3\gamma\rho^2} = -\frac{r_0\langle\beta_{\rm x,y}\rangle}{2\pi\beta^2}\frac{N}{\gamma\rho^2}\,. \tag{39}$$

A few salient features of the coherent tune shift:

- The force is linear in $\bar{x}$, so there is a coherent tune *shift* (for the unbunched beam under scrutiny).
- The $1/\gamma$ dependence of the tune shift stems from the fact that the charged particles induce the electrostatic field and thus generate a force proportional to their number, but independent of their mass, whereas the deflection of the beam by this force is inversely proportional to their mass $m_0\gamma$.
- The coherent tune shift is never positive.
- Note that a perfectly conducting beam pipe has been assumed here, for simplicity. The effects of a thin vacuum chamber with finite conductivity are more subtle [2].

### 3.3. The 'Laslett' coefficients

A rather realistic accelerator scenario is shown in Fig. 12: a beam with elliptic cross section travels with speed $\beta c$ through an elliptic vacuum chamber (ideal conductor) and between the ferromagnetic yokes of bending magnets. It is unbunched and has a uniform charge density (which is a less realistic assumption). For this and even simpler geometries — some of which are covered here — the incoherent and coherent tune shifts can be expressed in terms of the 'Laslett' coefficients [5] ($\varepsilon$ for incoherent, $\xi$ for coherent). The formulae below [Eq. (40)] are given for the vertical plane $y$; just replace $y$ by $x$ to get the horizontal results. The Laslett coefficients for simple geometries are compiled in Table 1.

$$\begin{aligned}\Delta Q_{\rm y,inc.} &= -\frac{Nr_0\langle\beta_{\rm y}\rangle}{\pi\beta^2\gamma}\left(\underbrace{\frac{\varepsilon_0^{\rm y}}{b^2\gamma^2}}_{\text{Direct}} + \underbrace{\frac{\varepsilon_0^{\rm y}}{h^2}}_{\text{electr. image}} + \underbrace{\beta^2\,\frac{\varepsilon_2^{\rm y}}{g^2}}_{\text{Magnetic image}}\right), \\ \Delta Q_{\rm y,coh.} &= -\frac{Nr_0\langle\beta_{\rm y}\rangle}{\pi\beta^2\gamma}\left(\frac{\xi_1^{\rm y}}{h^2} + \beta^2\,\frac{\xi_2^{\rm y}}{g^2}\right).\end{aligned} \tag{40}$$

Table 1: Laslett coefficients for incoherent ($\varepsilon$) and coherent ($\xi$) tune shifts, for simple geometries

| Laslett coefficients | Circular $(a = b,\ w = h)$ | Elliptical (e.g. $w = 2h$) | Parallel plates $(h/w$ = 0) |
|---|---|---|---|
| $\varepsilon_0^{\mathrm{x}}$ | 1/2 | $\frac{b^2}{a(a+b)}$ | |
| $\varepsilon_0^{\mathrm{y}}$ | 1/2 | $\frac{b}{a+b}$ | |
| $\varepsilon_1^{\mathrm{x}}$ | 0 | $-0.172$ | $-0.206$ |
| $\varepsilon_1^{\mathrm{y}}$ | 0 | 0.172 | 0.206 |
| $\xi_1^{\mathrm{x}}$ | 1/2 | 0.083 | 0 |
| $\xi_1^{\mathrm{y}}$ | 1/2 | 0.55 | 0.617($\pi^2$/16) |
| $\varepsilon_2^{\mathrm{x}}$ | $-0.411(-\pi^2/24)$ | $-0.411$ | $-0.411$ |
| $\varepsilon_2^{\mathrm{y}}$ | $0.411(\pi^2/24)$ | 0.411 | 0.411 |
| $\xi_2^{\mathrm{x}}$ | 0 | 0 | 0 |
| $\xi_2^{\mathrm{y}}$ | $0.617(\pi^2/16)$ | 0.617 | 0.617 |

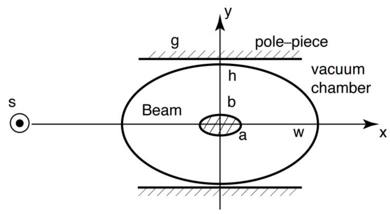


Fig. 12: A beam of elliptic cross section in an elliptic beam pipe and inside a ferromagnetic boundary (dipole magnet); the symbols are used in Table 1

For the elliptic geometry (see Fig. 12) with the vertical beam and vacuum chamber dimensions smaller than horizontally, which is quite common in realistic synchrotrons, most coefficients are larger vertically. Note also that the coherent coefficients $\xi$ are all positive or zero, that is the coherent tune shifts are negative (defocusing) or zero for all geometries, but never focusing.

## 4. TUNE SHIFT/SPREAD IN BUNCHED BEAMS

The arguments and formulae presented in the preceding sections apply to unbunched beams only. There is a class of accelerators where this exceptional situation indeed prevails: hadron (mostly ions or antiprotons) cooler rings or accumulators, where not too small intensities are cooled down to very small transverse emittances, mostly by electron cooling. As the direct space charge tune shift is proportional to the ratio intensity/emittance [the term $N/E$ in Eq. (19)], values of $\Delta Q \sim$ 0.1 to 0.2 can be reached in these cooling rings.

### 4.1. Comparison between unbunched and bunched beams

The majority of low-energy machines were built to accelerate particles, thus feature bunched beams. The fact that $N$ particles are no longer evenly distributed around the ring but are lumped in bunches aggravates space charge effects. This is illustrated in Fig. 13 where some basic features of unbunched beams (left column) are compared with bunched beams (right column).

The coasting beam is described by a constant line density $\lambda_0$, a band in the longitudinal phase plane of height $\Delta p$, and (for a 3-D uniform particle density) a $Q$-shift (–0.25 in this example). If this situation were realistic, one could readily correct this $Q$-shift by increasing the external betatron tune by 0.25, and space charge would not be an issue.

For a bunched beam (right-hand column in Fig. 13), the line density varies between 0 and $\hat{\lambda}$

with the average value $\bar{\lambda}$. Note that in low energy hadron synchrotrons, the bunch length is a few to many meters, whereas the transverse beam size is a few cm, so to a good approximation, a bunch consists of many longitudinal slices which behave independently of each other: the space charge tune shift of each slice depends on the local line density $\lambda(s)$. This causes a *tune spread* along the bunch, for *both incoherent* (direct space charge + images) and *coherent* tune shifts. The latter effect has been put forward to explain [6] the rather fast decoherence of a coherently oscillating high-intensity proton beam at injection into the CERN SPS at 26 GeV/$c$.

What happens to a single particle in the bunch? Each of them performs synchrotron oscillations which periodically vary its relative position $s$ and its momentum deviation $\Delta p$ in the longitudinal phase plane, with a period of typically 100 $\mu$s to a ms, lasting many machine revolutions. By this motion, the particle is driven back and forth in the bunch and periodically 'feels' different local line densities. The incoherent tune shift during a synchrotron oscillation period is shown in Fig. 13 for particles a,b,c with increasing synchrotron oscillation amplitudes: particle a stays near the bunch centre with its large line density and experiences large $Q$-shifts but small $Q$-variations during the oscillation, while particle c with its large amplitude synchrotron oscillation undergoes strong variations in $\Delta Q$ (from almost zero to –0.5 in this example). It is no longer possible to compensate space charge tune 'shifts' by adjusting the external focusing.

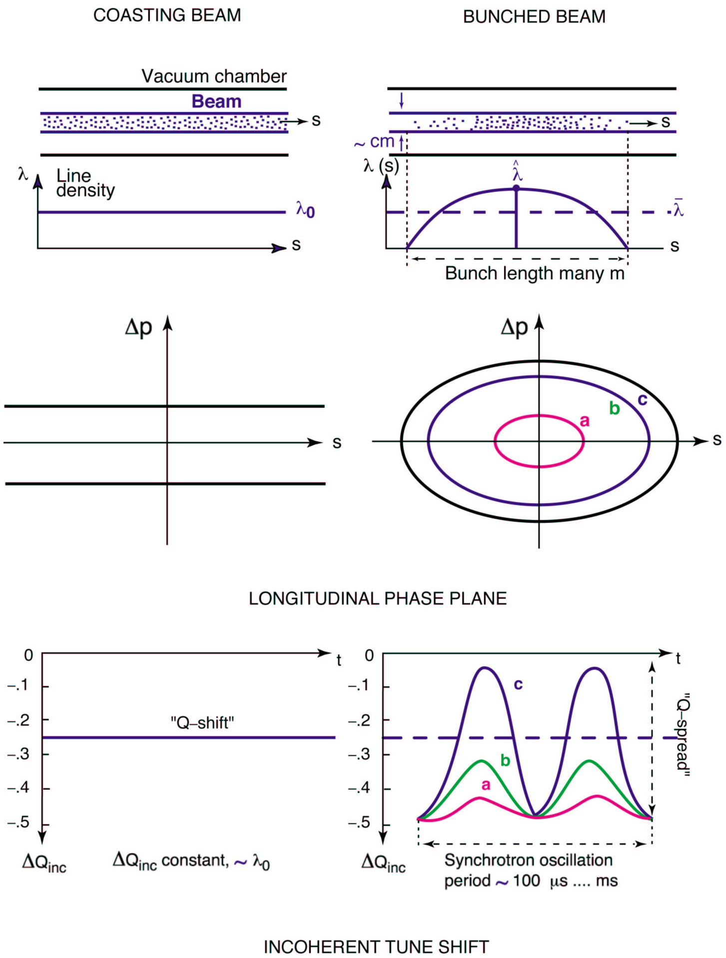


Fig. 13: Comparison between a coasting (unbunched) (left column) and a bunched beam (right column): particles in the beam pipe, line density $\lambda(s)$, longitudinal phase plane, $Q$-'shift' (from top to bottom).

### 4.2. Transverse space charge with bunched beams: a practical example [7]

The repercussions of bunched beams are illustrated with the CERN PS Booster, a space-charge dominated machine built for a tenfold increase of the CERN PS beam intensity. Figure 14 shows the tune diagram with all the low-order betatron resonances which are deemed to cause undesirable beam losses and beam emittance blow-up. The big 'necktie'-shaped area depicts the tune spread at 50 MeV (injection) with a total $\Delta Q_{\mathrm{y}}$ of about $-0.6$, which covers several dangerous non-linear resonances. Note that individual particles do not stay at constant tunes $Q_{\mathrm{x}}$, $Q_{\mathrm{y}}$ but are moved up and down in the necktie area, so they repetitively cross the low-order stopbands, and some of them will be lost. Fortunately $\Delta Q$ shrinks as the beam is accelerated by virtue of the $1/\beta^2\gamma^3$ term in Eq. (19); to profit from this feature, the machine tune is moved into an area clear of these stop-bands as soon as possible. Note that resonances above order 4 ($mQ_{\mathrm{x}} + nQ_{\mathrm{y}} = p$ with $|m| + |n| > 4$) can be ignored in this case because of the short acceleration time of 0.4 sec.

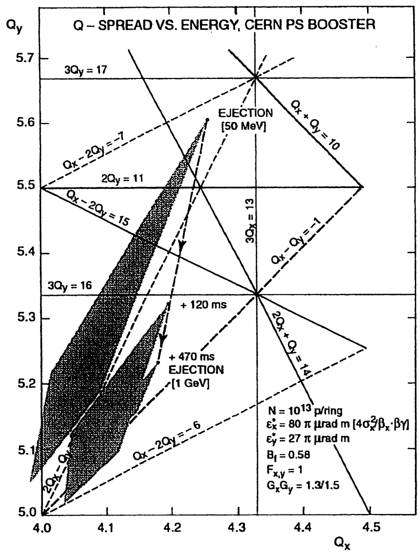


Fig. 14: Example for a space-charge limited synchrotron: betatron tune diagram and areas covered by direct space-charge tune spreads at injection, intermediate, and extraction energies for the CERN Proton Synchrotron Booster. During acceleration, space charge gets weaker and the 'necktie' area shrinks, enabling the external machine tunes to move the 'necktie' to an area clear of betatron resonances.

### 4.3. Incoherent tune shift: a practical formula

Starting with Eq. (25) for the vertical direct space charge tune shift of a uniformly charged beam with an elliptic cross section, one develops a more realistic formula for synchrotrons dominated by direct space charge by introducing various 'form factors'. Replacing $E_{\mathrm{x}}$ by $a^2/\beta_{\mathrm{x}}$, $E_{\mathrm{y}}$ by $b^2/\beta_{\mathrm{y}}$, one gets

$$\Delta Q_{\mathrm{y}} = -\frac{r_0}{\pi}\left(\frac{q^2}{A}\right)\frac{N}{\beta^2\gamma^3}\frac{F_{\mathrm{y}}\,G_{\mathrm{y}}}{B_{\mathrm{f}}}\left\langle\frac{\beta_{\mathrm{y}}}{b(a+b)}\right\rangle . \tag{41}$$

Evaluation of the average term and using $\langle\beta\rangle = R/Q$, the 'smooth approximation', yields

$$\left\langle\frac{\beta_{\mathrm{y}}}{b(a+b)}\right\rangle = \left\langle\frac{\beta_{\mathrm{y}}}{b^2\left(1+\frac{a}{b}\right)}\right\rangle \approx \frac{1}{E_{\mathrm{y}}\left(1+\sqrt{\frac{E_{\mathrm{x}}Q_{\mathrm{y}}}{E_{\mathrm{y}}Q_{\mathrm{x}}}}\right)} \tag{42}$$

and finally a formula for the incoherent tune shifts in either plane,

$$\Delta Q_{\mathrm{x,y}} = -\frac{r_0}{\pi}\left(\frac{q^2}{A}\right)\frac{N}{\beta^2\gamma^3}\frac{F_{\mathrm{x,y}}G_{\mathrm{x,y}}}{B_{\mathrm{f}}}\frac{1}{E_{\mathrm{x,y}}\left(1+\sqrt{\frac{E_{\mathrm{y,x}}Q_{\mathrm{x,y}}}{E_{\mathrm{x,y}}Q_{\mathrm{y,x}}}}\right)} \tag{43}$$

by inserting the following form factors:

- $F_{\mathrm{x,y}}$: form factor derived from Laslett's image coefficients for incoherent tune shifts, $\varepsilon^{\mathrm{x,y}}$ (Table 1)
- $G_{\mathrm{x,y}}$: form factor depending on the particle distribution in the transverse $x$-$y$ plane:
  $G$=1 uniform (for $E_{\mathrm{x,y}}$ containing 100% of the beam);
  $G$=2 Gaussian (for $E_{\mathrm{x,y}}$ containing 95% of the beam) (see Eq. 30);
  In general $1 < G < 2$.
- $B_{\mathrm{f}}$: Bunching factor, $B_{\mathrm{f}} = \bar{\lambda}/\hat{\lambda}$, mean/peak line density, 1 for unbunched, $< 1$ for bunched beams.

The term ($q^2/A$), where q is the charge state and $A$ the mass of ions, witnesses the strong space-charge forces prevailing in beams of high-charge-state ions at even low intensity $N$ (number of ions in beam).

### 4.4. How to overcome the 'space-charge limit'?

In Fig. 14, an example of a machine working in a heavy space-charge regime is presented. Incoherent tune shifts of beyond 0.5 can barely be tolerated without excessive particle loss, so for a given machine transverse acceptance, there is a hard intensity limit, the *space-charge limit*. What are the ways to overcome it? The essential parameters determining the tune shift are shown in the formula

$$\Delta Q \sim \frac{N}{E_{\mathrm{y}}\beta^2\gamma^3} \ .$$

Assume now that a large proton synchrotron is limited in $N$ because $\Delta Q$ reaches values around 0.5 when filling the (vertical) acceptance $E_{\mathrm{y}}$ which cannot be changed without rebuilding the machine. One sees that the only way to increase $N$ is then to raise $\beta^2\gamma^3$, that is the *injection energy*. This has indeed been done in the past in several laboratories, in the following ways:

- Make the linear accelerator (Linac) longer (FNAL): By adding more tanks, the proton energy was raised from 200 to 400 MeV, yielding a potential gain factor of 2.6 in $\beta^2\gamma^3$ and thus in the limit intensity the downstream synchrotron (in fact, the FNAL Booster) can digest: almost a factor 2 was achieved (Fig. 15).
- Add a small Booster synchrotron to raise the injection energy of the main ring. This was the strategy adopted by CERN (adding a four-ring Booster to the PS), and by BNL where a fast-cycling Booster was added to fill the AGS. Note that the circumference of the Booster has to be much smaller (factor 4 in both cases) to enable filling of the main ring. In both cases, the limiting intensity indeed was boosted dramatically, albeit less than the calculated factor (Fig. 16, Table 2).

Table 2: Intensity gain factors due to Booster synchrotrons added to the CERN PS and BNL AGS

| | Linac (MeV) | Booster (GeV) | $N = R/r$ | Potential gain in $N$ (by $\beta^2\gamma^3$) | Gain achieved |
|---|---|---|---|---|---|
| CERN PS | 50 | 1 | 4(rings) | 59 | $\sim$15 |
| BNL AGS | 200 | 1.5 | 4(batches) | 26 | $\sim$5 |

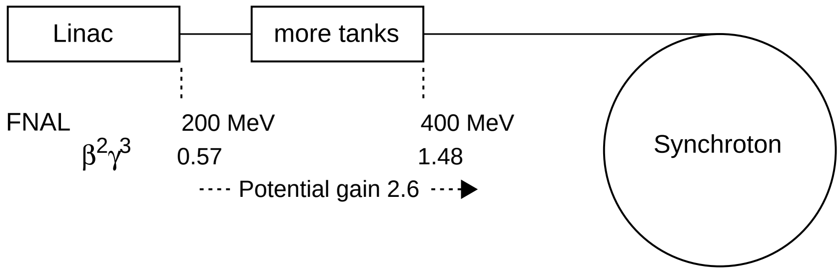


Fig. 15: Increasing the Linac energy at FNAL raises the limit intensity of the Booster synchrotron by almost a factor 2.

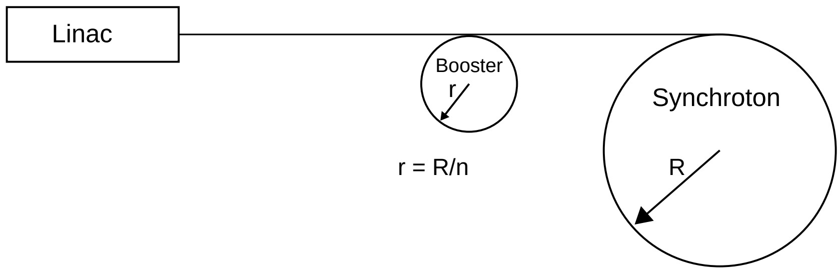


Fig. 16: Adding a smaller Booster synchrotron (1/4 of main ring circumference) boosts the limiting proton intensity: At CERN a four-ring, slow-cycling Booster fills the PS in one batch, whereas a fast-cycling Booster in BNL fills the AGS in four batches

# References


[1] A. Hofmann, *'Tune shifts from self fields and images'*, CAS Jyväskylä 1992, CERN 94–01, pp. 329–348.

[2] P.J. Bryant, *'Betatron frequency shift due to self and image fields'*, CAS Aarhus 1986, CERN 87–10, pp. 62–78.

[3] K. Schindl, *'Space charge'*, Proc. Joint US-CERN-Japan-Russia School on Particle Accelerators, Beam Measurements, Montreux, May 1998, edited by S. Kurokawa, S.Y. Lee, E. Perevedentsev, S. Turner, World Scientific, 1999, pp. 127–151.

[4] See for example J. Rossbach, P. Schmüser, *'Basic course on accelerator optics'*, CAS Jyväskylä 1992, CERN 94–01, p. 76.

[5] L.J. Laslett, *'On intensity limitations imposed by transverse space-charge effects in circular particle accelerators'*, Summer Study on Storage Rings, BNL Report 7534, p. 325–367.

[6] L. Vos, *'Decoherence from space charge'*, presented at the XVIIth Int. Conf. High Energy Part. Accel., Dubna, Russia, September 1998, Internal Report CERN SL–98–056 AP.

[7] J.P. Delahaye, G. Gelato, L. Magnani, G. Nassibian, F. Pedersen, K.H. Reich, K. Schindl, H. Schönauer, *'Shaping of proton distribution for raising the space-charge limit of the CERN PS Booster'*, Proc. 11th Intern. Conf. High Energy Accel., Geneva, July 1980, p. 299–304.